International Journal of Chemical, Materials and Biomolecular Sciences
ISSN: 2415-6620
Vol:11, No:1, 2017

Research of the Load Bearing Capacity of Inserts Embedded in CFRP under Different Loading Conditions

F. Pottmeyer, M. Weispfenning, K. A. Weidenmann

***Abstract*—**Continuous carbon fiber reinforced plastics (CFRP) exhibit a high application potential for lightweight structures due to their outstanding specific mechanical properties. Embedded metal elements, so-called inserts, can be used to join structural CFRP parts. Drilling of the components to be joined can be avoided using inserts. In consequence, no bearing stress is anticipated. This is a distinctive benefit of embedded inserts, since continuous CFRP have low shear and bearing strength. This paper aims at the investigation of the load bearing capacity after preinduced damages from impact tests and thermal-cycling. In addition, characterization of mechanical properties during dynamic high speed pull-out testing under different loading velocities was conducted. It has been shown that the load bearing capacity increases up to 100% for very high velocities (15 m/s) in comparison with quasi-static loading conditions (1.5 mm/min). Residual strength measurements identified the influence of thermal loading and preinduced mechanical damage. For both, the residual strength was evaluated afterwards by quasi-static pull-out tests. Taking into account the DIN EN 6038 a high decrease of force occurs at impact energy of 16 J with significant damage of the laminate. Lower impact energies of 6 J, 9 J, and 12 J do not decrease the measured residual strength, although the laminate is visibly damaged - distinguished by cracks on the rear side. To evaluate the influence of thermal loading, the specimens were placed in a climate chamber and were exposed to various numbers of temperature cycles. One cycle took 1.5 hours from -40 °C to +80 °C. It could be shown that already 10 temperature cycles decrease the load bearing capacity up to 20%. Further reduction of the residual strength with increasing number of thermal cycles was not observed. Thus, it implies that the maximum damage of the composite is already induced after 10 temperature cycles.

***Keywords*—**Composite, joining, inserts, dynamic loading, thermal loading, residual strength, impact.

I. Introduction

IN the field of transportation lightweight (e.g. automotive applications) structures with outstanding specific mechanical properties are needed to save resources. Due to this requirement, CFRP structures feature high application potential. Mechanical fasteners offer the possibility to allow for an inexpensive, detachable connection of these typically thin-walled CFRP parts to metal-based structures in the context of multi-material design [1]. In many cases, the mechanical joining (e.g. rivets and bolts) of these (continuous) CFRP parts is related to drilling before fastening which leads to inevitable bearing stress concentrations in the laminate [2]. This effect causes a degradation of the performance since CFRP have low bearing strength [3], [4]. Remedy for this problem is the use of embedded metal elements, so-called inserts. They usually consist of a boundary plate with a welded bushing. With the help of inserts, it is possible to maintain the fiber continuity. In addition, drilling of the components – and hence cutting of the load-bearing fibers – to be joined can be avoided [5]. Previous investigations of inserts embedded in CFRP are only regarding the maximum forces or torques under quasi-static loading conditions for getting information about the load bearing capacity. Ferret et al. [6] investigated two different types of bigHead® inserts under tensile (pull-out), bending as well as compressive (push-in) loads. Increased tensile strength was observed for inserts with smaller boundary plate. The authors observed that final failure was caused by the fracture of large inserts. This fracture was located around the insert's stud so the design of the larger inserts reduced tensile strength. Hopmann et al. [7] also performed pull-out tests to compare the performance of inserts and bonded fasteners (so-called onserts). It has been shown that the performance of inserts was up to 37% higher. Fleischer and Gebhardt [8] tested inserts with different types of surface treatments under different loading conditions. The performance was improved up to 42% by generating pins on the lower side of the boundary plate by additive manufacturing. With the help of thermal (arc) spraying of the boundary plates, the bending strength was enhanced up to 41% due to the extremely rough surface. Schwarz et al. [9] investigated the influence of geometrical and manufacturing parameters on the performance of embedded inserts under bending loads. Own preliminary work [10] deals with the testing of embedded inserts under bending, torsion, shear, compressive and tensile loads. The latter was identified to be the most critical load case. Subsequent pull-out tests with a geometrical parameter variation showed that thicker metal sheets of the inserts and thicker laminates can enhance the performance significantly. Further work [11] deals with the investigation of the damage evolution including the deformation of the insert using in-situ CT analysis. For that purpose, embedded inserts were tested under the abovementioned critical tensile load. It could be shown that the beginning and the growth of the de-bonding of the insert can be well reproduced. This de-bonding is responsible for the

F. Pottmeyer is with the Karlsruher Institute of Technology, Institute for Applied Materials IAM-WK, 76131 Karlsruhe (phone: +49 721 608 - 47441; fax: +49 721 608 - 48044; e-mail: florentin.pottmeyer@kit.edu).

M. Weispfenning and K. A. Weidenmann are with the Karlsruher Institute of Technology, Institute for Applied Materials IAM-WK, 76131 Karlsruhe (e-mail: ukdob@student.kit.edu, kay.weidenmann@kit.edu).

high decrease of force observed in pull-out tests. As the literature survey given above indicates, there are only investigations dealing with the load bearing capacity of inserts under different types of quasi-static loading conditions so far. Consequently, there are no works investigating the load bearing capacity of inserts under dynamic, thermal, or predamaged loading conditions. This paper deals with the investigation of the load bearing capacity of embedded inserts tested with different crosshead velocities to evaluate a possible strain-rate dependency. Furthermore, residual strength measurements of thermal loaded and predamaged embedded inserts were carried out. These measurements comprise the quasi-static load bearing capacity after preinduced damages from impact tests or thermal-cycling. Residual strength measurements after thermal loading and preinduced damage as well as dynamic tests have been investigated comprehensively with single CFRP so far, but have not been performed with inserts. Taniguchi et al. [12] tested unidirectional CFRP laminates under high strain rates and demonstrated that the tensile modulus and strength in longitudinal direction are independent of the strain rate. But, the same tensile properties increased with rising strain rate when tested in the transverse direction. Similar results were confirmed by Harding and Welsh [13]. The measurement of the residual strength is common in CFRP sandwich panels [14], [15] or laminates [16], [17]. Caprino [18] performed residual tensile strength measurements after impacting CFRP laminates with energies up to 4.3 J. The residual tensile strengths of the predamaged specimens were reduced up to 60%. Sánchez-Sáez et al. [19] investigated the compressive residual strength of different types of CFRP lay-ups after impacts with a maximum energy of 13 J. Compression after impact tests were conducted afterwards at low temperatures (-60 °C and -150 °C) and compared to same tests at room temperature. With higher impact energies the residual strength significantly declined to a minimum which rather stayed constant even with further increased energies. The cross-ply laminate showed the worst damage tolerance at all impact energies and temperatures. Shimokawa et al. [20] found microcracks in CFRP loaded even in the first ten thermal cycles (-54 °C to 177 °C with each retention time at 15 minutes). Although the number of microcracks increased up to 10.000 cycles no degradation of compressive strength was observed. The value of the nominal strength was similar if loaded between 1.000 and 10.000 cycles.

II. Experimental

A. Materials and Specimen Geometry

The specimens consist of a flat CFRP plate with one centrally positioned insert in the center of the laminate. The same sample geometry has been chosen in [21], [5], [8], [10], [11] and allows for a comparison of the results. An exemplary picture with the appropriate dimensions can be seen in Fig. 1.

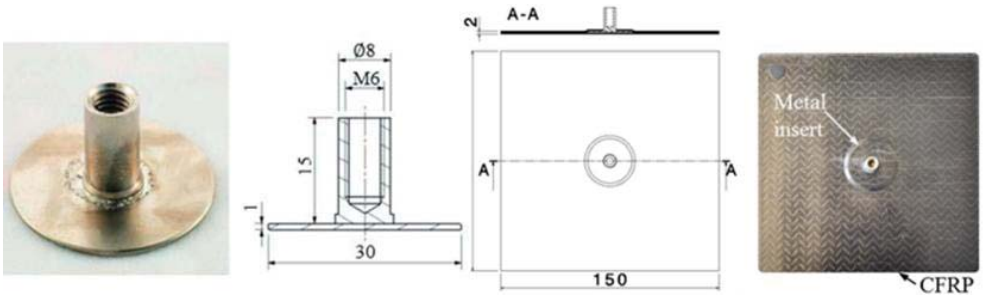

Fig. 1 Exemplary picture and dimensions of the metal insert and CFRP specimen

The CFRP is built from eight plies of a multiaxial non-woven carbon fiber fabric (Hexcel NLT00 series, 0°/90°, 200 g/m²) resulting in a fiber volume fracture of 0.44. The matrix is an epoxy resin manufactured by Sika® (Biresin® CR170/CH150-3). The manufacturing of the insert is done by stud welding a threaded bolt on a flat metal sheet (boundary plate). Both components are made of stainless steel (1.4301) to prevent corrosion. After welding, the insert is embedded during the preforming process between the four lower and four upper plies of the carbon fiber fabric. The fibers are guided around the bolt to maintain the fiber continuity. The specimens are finally manufactured in a resin transfer molding (RTM) process at the Institute of Production Science (wbk) at KIT, where the infiltration is carried out on a hydraulic press (Lauffer type RP 400) using a flow metering and mixing machine (Tartler Nodopur VS-2K). The curing is at 70 °C for 60 minutes and the infiltration pressure is set to 9 bar.

B. Test Setup and Procedure

The tensile tests were carried out on two different testing machines depending on the strain rates to be investigated. The reference specimens were tested with a crosshead velocity of 1.5 mm/min on a universal testing machine of Zwick. The velocity of 150 mm/min was also carried out on this machine. The experimental setup and the section of the test device are shown in Fig. 2. An inductive strain gauge (ISG) is additionally installed underneath the specimen to measure the deflection of the lower side of the laminate. The same mounting frame is installed on a testing machine of Zwick (HTM5020) to carry out the high-speed crosshead-velocities of 250 mm/s and 15 m/s. The forces and (traverse-) displacements were measured and evaluated. The load bearing capacity is defined as the maximum force for both testing methods. At least five specimens of each loading condition were tested.

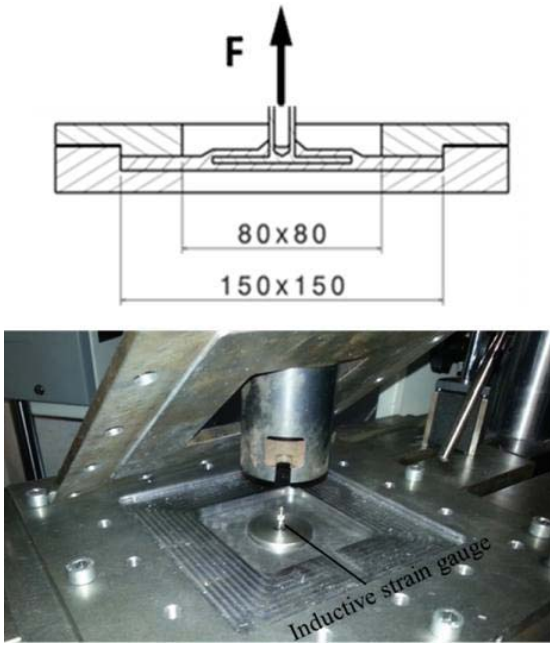

Fig. 2 Experimental setup and section of the test device [10], bottom: inductive strain gauge (ISG)

Preinduced damage of the specimens was performed by high-speed indenting using a drop tower of Instron dynatup shown in Fig. 3.

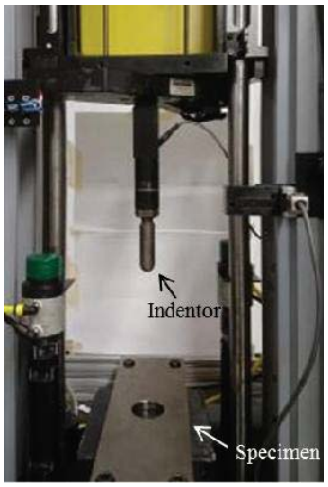

Fig. 3 Drop tower of Instron with clamped specimen and indentor

Changing the height of the indention weight leads to different indention energies. Taking into account the DIN EN 6038 the energies were set to 6 J, 9 J, 12 J, and 16. After impacting, the residual strength measurement was conducted with a crosshead-velocity of 1.5 mm/min on the setup shown in Fig. **2**. In addition, specimens were also thermal loaded using a climate chamber of Vötsch. Therefore, temperature cycles (10, 100 and 1000) shown in Fig. 4 were conducted starting at room temperature. The residual strength after impact was measured analogous as for the undamaged reference specimens.

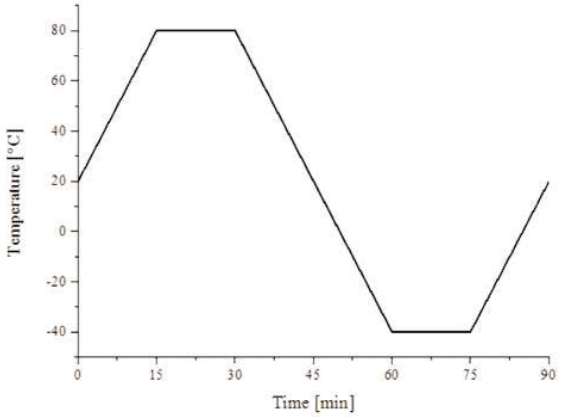

Fig. 4 One temperature cycle for the thermal loading

The reference specimen for all loading conditions is tested quasi-static with 1.5 mm/min and neither predamaged nor thermally loaded.

III. Results

A. Dynamic Pull-Out Test

The force-/displacement curve of the reference (1.5 mm/min) is shown in Fig. 5. The blue curve corresponds to the centrally installed ISG. As can be seen, the slope of the ISG decreases at approximately 4.5 mm (traverse) displacement and 3800 N. The course of the ISG also drops at 4000 N, where the first remarkable decrease of force occurs. The post-mortem picture including the typical crosswise cracks around the stud is shown in Fig. 6.

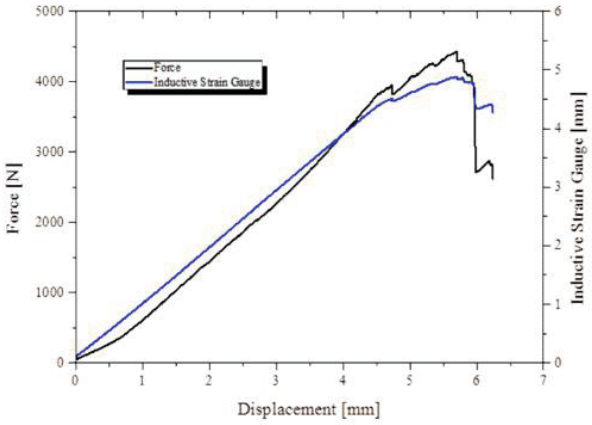

Fig. 5 Force-/displacement diagram of a specimen tested with 1.5 mm/min

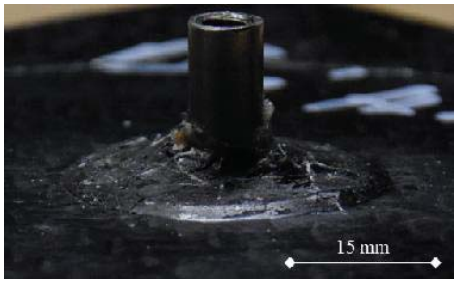

Fig. 6 Post-mortem picture of a specimen tested with 1.5 mm/min

The force-displacement curve of a specimen tested with 150 mm/min is shown in Fig. 7. Here, the value of the ISG drops suddenly at a displacement of approximately 6 mm. The course of the test curve is not characterized by many decreases in forces. Fig. 8 contains the post-mortem picture. Here, breakage of fiber bundles can be seen instead of single fiber fracture.

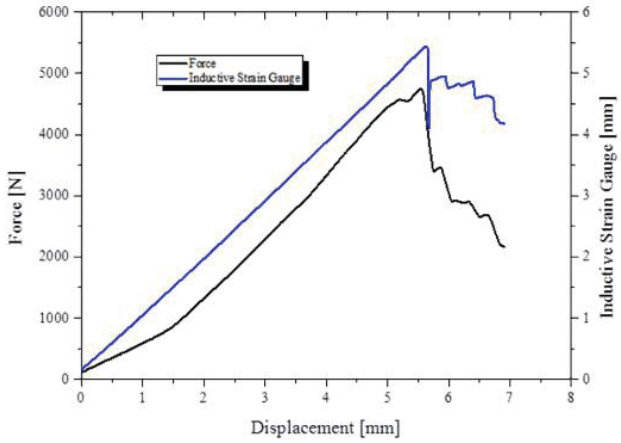

Fig. 7 Force-/displacement diagram of a specimen tested with 150 mm/min

Fig. 8 Post-mortem picture of a specimen tested with 150 mm/min

The high speed pull-out tests were carried out on another testing machine with different stiffness and measurement of traverse displacements. Final failure was always initiated by pulling out the insert of the laminate.

The results of the pull-out test with 250 mm/s are shown in Fig. 9. The measured signal is characterized by a superimposition of oscillations of the piezo-driven load cell and the ongoing damage evolution. The last decrease of force at 5.5 mm displacement resulted in a high increase of force to more than 5000 N, which is probably caused by the final failure.

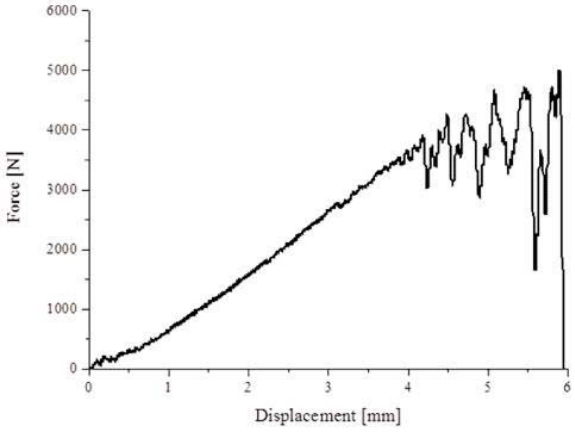

Fig. 9 Force-/displacement diagram of a specimen tested with 250 mm/s

The high speed crosshead velocity was set to 15 m/s. The result is shown in Fig. 10. The oscillations of the piezo-driven load cell are not depicted, since they occurred only after final failure.

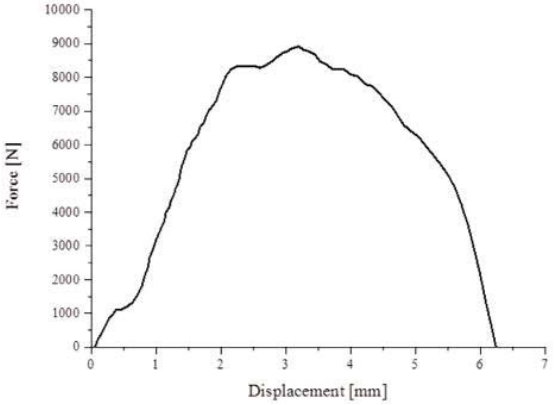

Fig. 10 Force-/displacement diagram of a specimen tested with 15 m/s

The failure of both specimens is characterized by delamination and pulling-out the insert of the laminate. Fig. 11 contains both deformed inserts after testing to evaluate the degree of deformation.

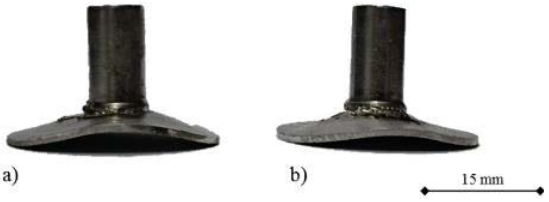

Fig. 11 Post-mortem picture of the deformed inserts with a) 250 mm/s and b) 15 m/s

Fig. 12 gives an overview of the load bearing capacity with the different tested crosshead velocities. The load bearing capacity increases linearly with the crosshead velocity up to 250 mm/s. Carrying out high-speed pull-out tests with 15 m/s a steep increase of the load bearing capacity can be observed.

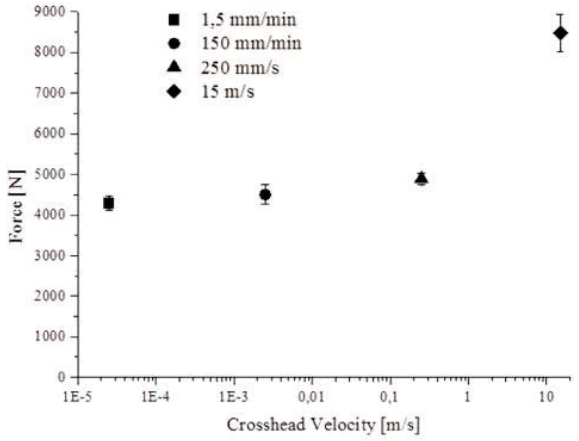

Fig. 12 Load bearing capacities of all tested crosshead velocities

B. Residual Strength of Thermal Loaded Specimens

The specimens were thermally loaded with a different number of thermal cycles (cf. Fig. 4). The residual strength was measured on the universal testing machine of Zwick (cf. Fig. 2) with a crosshead velocity of 1.5 mm/min. The force-displacements curves are similar for all tested specimens. Fig. 13 gives an overview of the load bearing capacities depending on the number of thermal cycles. The load bearing capacity already decreases after 10 thermal cycles and stays constant even with increasing number of thermal cycles.

The post-mortem pictures of all specimens after thermal loading show an analogous damage behavior as the reference specimens (cf. Fig. 6).

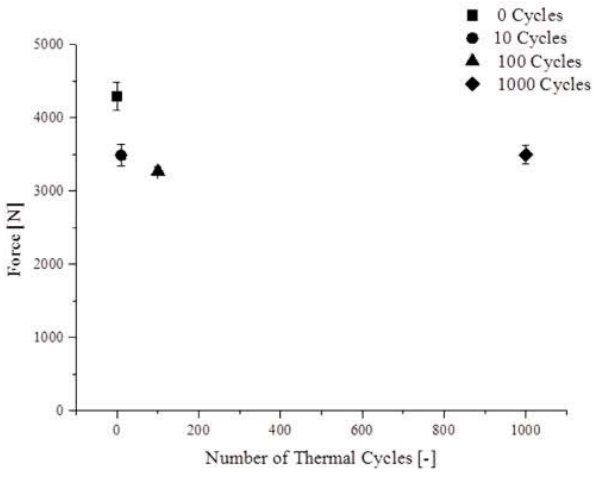

Fig. 13 Load bearing capacities of all performed number of thermal cycles

C. Residual Strength of Predamaged Specimens

The specimens were predamaged with an indentor (drop weight 5 kg) accelerated by a drop tower (e.g. Fig. 3). The impact energies of 6 J, 9 J, 12 J, and 16 J were performed aligning the height of the indentor. The residual strength was measured the same way as the thermal loaded specimens after impacting. Before this, the predamaged specimens were scanned by using µ-computed tomography to evaluate the accompanied damage. Fig. 14 gives an overview of the preinduced damage of the specimens impacted with different energies.

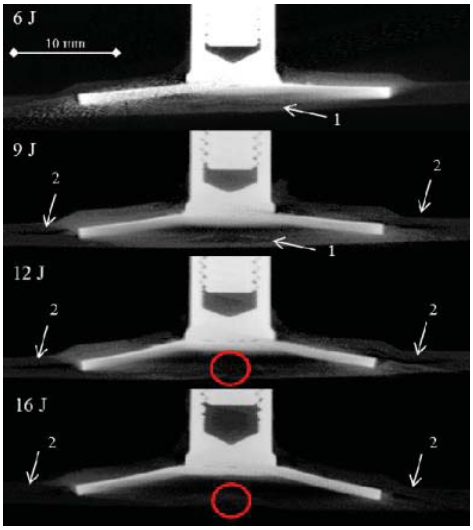

Fig. 14 CT scans of the predamaged specimens with fiber cracks (1), delamination (2) and extensive fiber breakage (red circle)

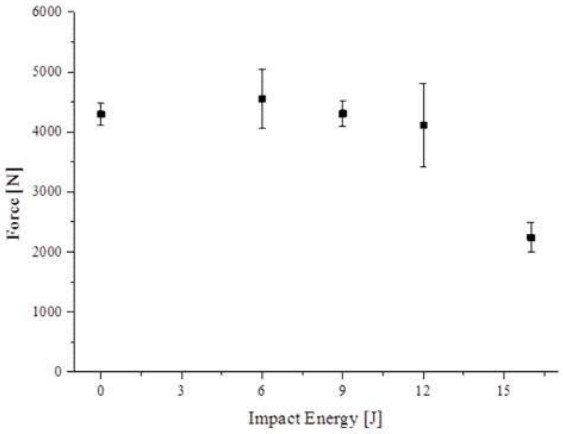

Fig. 15 Load bearing capacities of all performed impact energies

6 J is enough energy to cause cracks in the laminate underneath the insert (1). Increasing the impact energy up to 9 J the insert is already partially de-bonded from the laminate which can be seen in a resulting gap between insert and laminate. This causes a deformation of the insert as well. In addition, cracks in the laminate (probably delamination) arise around the boundary plate of the insert (2). The breakage of

the lower side of the laminate (red circle) as well as the degree of deformation of the insert increases with the impact energy. An overview of the load bearing capacities depending on the impact energies is shown in Fig. 15. The load bearing capacities do not significantly differ between 0 and 12 J. The standard deviation is wider at specimens predamaged with 6 and 12 J. The impact energy of 16 J causes a decrease of the load bearing capacity to 50%. The post-mortem pictures of the residual strength measurements of all predamaged specimens are similar.

IV. Discussion

A. Dynamic Pull-Out Test

As can be seen in the overview of Fig. 12, the load bearing capacity improves with increasing crosshead velocity. The load bearing capacity is enhanced up to 100% performing a pull-out test with 15 m/s instead of 1.5 mm/s. Comparing the specimens tested with an ISG it is noticeable that the curve of the ISG is characterized by a sudden drop concerning the crosshead velocity of 150 mm/min, whereas the curve of the ISG with 1.5 mm/min decreases slightly. The ISG measures the deflection of the lower side of the laminate. As soon as the slope of the ISG decreases, a relative movement between insert and laminate has to happen and indicates onset of de-bonding at the interface between laminate and insert. A drop of the curve of the ISG mainly indicates to a sudden de-bonding of the insert. This leads to the assumption that the interface insert/laminate is dependent on the crosshead velocity. The normal strength of the interface is enhanced performing pull-out tests with higher crosshead velocities. This can also be seen in the post-mortem pictures of the abovementioned specimens. Breakage of fiber bundles instead of single fiber fracture can be observed in specimen tested with 150 mm/min (cf. Fig. 8). The fact is that the interface which fails suddenly, causes the fiber bundle breakage. Another evidence to confirm this assumption can be seen in Fig. 11. The plastic deformation of the insert decreases with increasing crosshead velocity from 0.25 to 15 m/s. This underlines the assumption of a strain rate sensitive interface de-bonding. Many investigations reveal that the strength of CFRPs is independent of the strain rate. However, this is not the case for matrix strength [12], [13], [22]. The tensile strength of CFRP laminates tested in the transverse direction was investigated by Taniguchi et al. [12]. The authors performed strain rates of 1.04×10^{-4} 1/s and 100 1/s which corresponds to crosshead velocities of 0.156 mm/min and 2.5 m/s, respectively. Here, the tensile strength increased linearly with the strain rate up to 17.8% which confirmed the strain rate dependency of the matrix. In the present work, the interface insert/laminate consists of epoxy resin. The load bearing capacity increases linearly up to 14% until the crosshead velocity of 250 mm/s. So, the present results match the literature at least quantitatively. Performing very high crosshead velocities cause a steep increase of the load bearing capacity.

B. Residual Strength of Thermal Loaded Specimens

The load bearing capacities after thermal loading are summarized in Fig. 13. It is notable that the residual strength stagnates already after 10 conducted thermal cycles. The load bearing capacity is nearly the same after 10, 100 or 1000 thermal cycles and approximately 20 % lower than the reference. After the manufacturing, residual stresses always arise in a CFRP laminate due to the higher shrinkage of the matrix compared with the fiber. Hybrid CFRP specimens with an adhesive bonding are characterized by a high mismatch in coefficient of thermal expansion (e.g. steel and CFRP). This leads to additional, significant residual stresses [23]-[25]. The magnitude of residual stress is sufficient to initiate matrix cracks [26], [27]. If a specimen is thermal loaded, the residual stresses increase as the difference between the operating temperature and the stress-free temperature increases [28], [29]. This stress-free temperature of the adhesive is similar to its curing temperature [30]-[32]. Shimokawa et al. [20] investigated the residual strength and the number of microcracks after thermal loaded CFRP. The authors found microcracks resulting of internal thermal stresses in CFRP in the first ten cycles. Although the number of microcracks increased up to 10.000 cycles, no degradation of residual strength was observed. So the value of the residual strength was constant between 1.000 and 10.000 cycles. Ju and Morgan confirmed in [29] that microcracks increased with the number of thermal cycles in CFRP laminates. Referring to [30]-[32], it can be assumed that the stress-free temperature of the specimens used is similar to the curing temperature of 70 °C. The minimum temperature of the thermal cycle is -40 °C causing increasing residual stresses and subsequent interfacial microcracks. It can be assumed that the number of microcracks increase with the number of thermal cycles. This relation, according to [20], did not affect the residual strength of the composite. In addition, the standard deviations are very low for all specimens.

C. Residual Strength of Predamaged Specimens

Fig. 15 gives an overview of the measured load bearing capacities of the predamaged specimens. Remarkable is the fact that the residual strength does not significantly decrease when impacting the specimens up to 12 J. Though the interface as well as the insert itself of the predamaged specimens are visibly damaged (cf. Fig. 14). In addition, impacting the specimens caused interlaminar fiber cracks around the boundary plate of the insert. Impacting a specimen with 16 J causes a decrease of the residual strength up to 50%. Comparing to literature the presented residual strengths of the embedded inserts remain high compared to [18]. Here, impacting CFRP laminates with 4.3 J causes reductions up to 60% of residual tensile strength. Sánchez-Sáez et al. [19] confirmed that due to increasing of impact energies (up to 13 J), the residual strength significantly decreased to a constant value at higher energies. In addition, cross-ply laminates showed the worst damage tolerance at all impact energies and temperatures. Here, also the standard deviation is very high

especially at energies of 6 J and 12 J, whereby the standard deviation of specimens impacted with 16 J is relatively small.

V. Conclusion

Investigations of the influence of different loading conditions on the load bearing capacity of embedded inserts have been carried out. Therefore, all specimens were tested under the critical tensile load case [10], performed via pull-out test.

The first loading condition comprises the dynamic pull-out test with increasing crosshead velocities. It could be shown that the load bearing capacity strongly depends on the crosshead velocity of the pull-out test. Increasing the velocity from 1.5 mm/min to 15 m/s improves the maximum force up to 100%. The failure behavior including the insert's deformation as well as the degree of fiber breakage shows a dependency too. The essential reason for this could be the fact that the interface insert/laminate consisting of the epoxy resin depends on the crosshead velocity. Hence, the specimen tested with 1.5 mm/min shows a progressive failure behavior of the interface, whereby the specimen tested with 150 mm/min is characterized by a sudden de-bonding of the insert.

Secondly, the residual strength was measured via the pull-out tests after thermal loading. Therefore, a different number of thermal cycles (10. 100 and 1000) were conducted. The residual strength decreases up to 20% performing 10 cycles but did not decrease further after 100 or 1000 cycles. A reason for this behavior could not be clarified doubtless, but concerning literature, it can be assumed that microcracks arise at the beginning of the thermal cycle in the interface insert/laminate. It can be further assumed that the density of these microcracks increases with increasing number of cycles.

Residual strength measurements were also performed with predamaged specimens. The specimens were impacted with different energies using a drop tower. The energies were set to 6 J, 9 J, 12 J, and 16 J. Comparing to the not-predamaged specimens, the residual strength of the specimens of 6–12 J did not significantly decrease though the insert as well as the laminate were obviously damaged.

Acknowledgment

This paper is based on investigations of the subproject 3 – "Fundamental research of intrinsically produced FRP-/metal-composites – from embedded insert to load bearing hybrid structure" – of the priority program 1712 "Intrinsic hybrid composites for lightweight load-bearings", which is kindly supported by the German Research Foundation (DFG). The authors kindly acknowledge the Institute for Production Science (wbk) at KIT for the manufacturing of the specimens within the cooperation in the abovementioned subproject.

References

[1] P. P. Camanho; M. Lambert: A design methodology for mechanically fastened joints in laminated composite materials. In: *Composites Science and Technology* 66 (15), S. 3004–3020, 2006.

[2] I. Eriksson: On the Bearing Strength of Bolted Graphite/Epoxy Laminates. In: *Journal of Composite Materials* 24 (12), S. 1246–1269, 1990.

[3] Yi Xiao; Takashi Ishikawa: Bearing strength and failure behavior of bolted composite joints (part I. Experimental investigation). In: *Composites Science and Technology* 65 (7-8), S. 1022–1031, 2005.

[4] B. Kolesnikov; L. Herbeck; A. Fink: CFRP/titanium hybrid material for improving composite bolted joints. In: *Composite Structures* 83 (4), S. 368–380, 2008.

[5] J. Gebhardt; J. Fleischer: Experimental Investigation and Performance Enhancement of Inserts in Composite Parts. In: *Procedia CIRP* 23, S. 7–12, 2014.

[6] B. Ferret; C. Anduze; C. Nardari: Metal inserts in structural composite materials manufactured by RTM. In: *Composites Part A* (29), S. 693–700, 1998.

[7] C. Hopmann; Fecher, M. L., Lineman, L.; R. Bastian; T. Gries; A. Schnabel; C. Greb: Comparison of the properties of Onserts and Inserts for a high volume production of structural composite parts. In: *Journal of Plastics Technology* 9 (4), S. 179–206, 2013.

[8] J. Fleischer; J. Gebhardt: Experimental Investigation of Metal Inserts Embedded in Composite Parts Manufactured by the RTM Process. 13th Japan International SAMPE Symposium and Exhibition,Nagoya, Japan, 2013.

[9] Marcus Schwarz; Michael Magin; Carsten Peil; Helmut Schürmann: Thin-walled FRP-laminates and local bending moments - incompatible or solvable by a skillful design? Internationale Tagung für Verstärkte Kunststoffe und Duroplastische Formmasse, Baden-Baden, Germany, 2004.

[10] Johannes Gebhardt; Florentin Pottmeyer; Jürgen Fleischer; Kay Weidenmann: Characterization of Metal Inserts Embedded in Carbon Fiber Reinforced Plastics. In: *MSF* 825-826, S. 506–513, 2015.

[11] Florentin Pottmeyer; Julia Bittner; Pascal Pinter; Kay André Weidenmann: In-situ CT damage analysis of metal inserts embedded in carbon fiber reinforced plastics. Submitted. In: *NDT & E International* 2016.

[12] Norihiko Taniguchi; Tsuyoshi Nishiwaki; Hiroyuki Kawada: Tensile strength of unidirectional CFRP laminate under high strain rate. In: *Advanced Composite Materials* 16 (2), S. 167–180, 2007.

[13] J. Harding; L. M. Welsh: A tensile testing technique for fibre-reinforced composites at impact rates of strain. In: *J Mater Sci* 18 (6), S. 1810–1826, 1983.

[14] Bing Wang; Lin-Zhi Wu; Li Ma; Ji-Cai Feng: Low-velocity impact characteristics and residual tensile strength of carbon fiber composite lattice core sandwich structures. In: *Composites Part B: Engineering* 42 (4), S. 891–897, 2011.

[15] G. Caprino; R. Teti: Impact and post-impact behavior of foam core sandwich structures. In: *Composite Structures* 29 (1), S. 47–55, 1994.

[16] V. J. Hawyes; P. T. Curtis; C. Soutis: Effect of impact damage on the compressive response of composite laminates. In: *Composites Part A: Applied Science and Manufacturing* 32 (9), S. 1263–1270, 2001.

[17] O. Ishai; A. Shragai: Effect of impact loading on damage and Residual Compressive Strength of CFRP laminated beams. In: *Composite Structures* 14 (4), S. 319–337, 1990.

[18] G. Caprino: Residual Strength Prediction of Impacted CFRP Laminates. In: *Journal of Composite Materials* 18 (6), S. 508–518, 1984.

[19] S. Sánchez-Sáez; E. Barbero; C. Navarro: Compressive residual strength at low temperatures of composite laminates subjected to low-velocity impacts. In: *Composite Structures* 85 (3), S. 226–232, 2008.

[20] T. Shimokawa; H. Katoh; Y. Hamaguchi; S. Sanbongi; H. Mizuno; H. Nakamura et al.: Effect of Thermal Cycling on Microcracking and Strength Degradation of High-Temperature Polymer Composite Materials for Use in Next-Generation SST Structures. In: *Journal of Composite Materials* 36 (7), S. 885–895, 2002.

[21] Jonas Wilkening; Florentin Pottmeyer; Kay André Weidenmann: Research on the interfering effect of metal inserts in carbon fiber reinforced plastics manufactured by the RTM process. 17th European Conference on Composite Materials, Munich, Germany, 2016.

[22] Yasushi Miyano; Masayuki Nakada; Hiroshi Kudoh; Rokuro Muki: Prediction of tensile fatigue life under temperature environment for unidirectional CFRP. In: *Advanced Composite Materials* 8 (3), S. 235–246, 1999.

[23] Patricia P. Parlevliet; Harald E.N. Bersee; Adriaan Beukers: Residual stresses in thermoplastic composites—A study of the literature—Part I. Formation of residual stresses. In: *Composites Part A: Applied Science and Manufacturing* 37 (11), S. 1847–1857, 2006.

[24] Kum Cheol Shin; Jung Ju Lee: Effects of thermal residual stresses on failure of co-cured lap joints with steel and carbon fiber–epoxy

composite adherends under static and fatigue tensile loads. In: *Composites Part A: Applied Science and Manufacturing* 37 (3), S. 476–487, 2006.

[25] Hak Sung Kim; Sang Wook Park; Dai Gil Lee: Smart cure cycle with cooling and reheating for co-cure bonded steel/carbon epoxy composite hybrid structures for reducing thermal residual stress. In: *Composites Part A: Applied Science and Manufacturing* 37 (10), S. 1708–1721, 2006.

[26] T. A. Bogetti; J. W. Gillespie: Process-Induced Stress and Deformation in Thick-Section Thermoset Composite Laminates. In: *Journal of Composite Materials* 26 (5), S. 626–660, 1992.

[27] John F. Timmerman; Matthew S. Tillman; Brian S. Hayes; James C. Seferis: Matrix and fiber influences on the cryogenic microcracking of carbon fiber/epoxy composites. In: *Composites Part A: Applied Science and Manufacturing* 33 (3), S. 323–329, 2002.

[28] Lucas F. M. da Silva; R. D. Adams: Stress-free temperature in a mixed-adhesive joint. In: *Journal of Adhesion Science and Technology* 20 (15), S. 1705–1726, 2006.

[29] J. Ju: Characterization of Microcrack Development in BMI-Carbon Fiber Composite under Stress and Thermal Cycling. In: *Journal of Composite Materials* 38 (22), S. 2007–2024, 2004.

[30] L. J. Hart-Smith: Adhesive-bonded double-lap joints. Hg. v. NASA CR-112235. NASA. Houston, Texas, 1973.

[31] F. S. Jumbo; I. A. Ashcroft; A. D. Crocombe; M.M Abdel Wahab: Thermal residual stress analysis of epoxy bi-material laminates and bonded joints. In: *International Journal of Adhesion and Adhesives* 30 (7), S. 523–538, 2010.

[32] Y. Yu; I. A. Ashcroft; G. Swallowe: An experimental investigation of residual stresses in an epoxy–steel laminate. In: *International Journal of Adhesion and Adhesives* 26 (7), S. 511–519, 2006.